

QUASI-STATIC INFLUENCE LINE IDENTIFICATION AND DAMAGE IDENTIFICATION OF EQUAL-SPAN BRIDGES BASED ON MEASURED VEHICLE-INDUCED DEFLECTION

KANG YANG¹, YOU LIANG DING^{1*}, HAN WEI ZHAO¹,
FANG FANG GENG², ZHEN SUN³

¹*School of Civil Engineering, Key Laboratory of C&PC Structures of the Ministry of Education, Southeast Univ., Nanjing 210096, China*

²*School of Architecture Engineering, Nanjing Institute of Technology, Nanjing 211167, China*

³*Faculty of Engineering (FEUP), University of Porto, R. Dr. Roberto Frias, 4200-465 Porto, Portugal.*

Received 18 June 2020; accepted 2 August 2021

Abstract. The bridge influence line (IL) reflects the response of a certain section due to varying load positions. As a result, IL has a wide application prospect in damage identification and condition assessment. Up to date, studies regarding IL have been focused on the structure condition evaluation. A feasible and practical method for damage identification is still not yet available. The present paper proposes a comprehensive damage identification methodology

* Corresponding author. E-mail: civilding@seu.edu.cn

Kang YANG (ORCID ID 0000-0002-4208-2580)
Youliang DING (ORCID ID 0000-0002-0774-426X)
Hanwei ZHAO (ORCID ID 0000-0002-7622-7784)
Fangfang GENG (ORCID ID 0000-0003-3118-3789)
Zhen SUN (ORCID ID 0000-0002-2053-4902)

Copyright © 2022 The Author(s). Published by RTU Press

This is an Open Access article distributed under the terms of the Creative Commons Attribution License (<http://creativecommons.org/licenses/by/4.0/>), which permits unrestricted use, distribution, and reproduction in any medium, provided the original author and source are credited.

based on IL under a moving vehicle is composed of data pre-processing, IL extraction, and damage detection. Firstly, a thorough review of existing IL identification methods based on signal processing is provided. Then three quasi-static IL identification methods based on measured data are discussed. Consequently, the study proposes a two-stage damage identification approach for simply supported bridges with equal span length. Also, the effectiveness of this approach is verified through field tests on a real girder bridge. At last, conclusions are drawn, and potential issues for the application of the proposed method in practice are discussed.

Keywords: damage identification, deflection, dynamic displacement IL, equal-span bridges, influence line, vehicle loads.

Introduction

The bridge is the “throat” of the traffic line, consequently, ensuring its safe and stable service is of great significance (Liu et al., 2016). The combination of internal and external influences will inevitably lead to a gradual deterioration in the service performance of the bridge. According to the latest statistics of the Ministry of Transport of RC China, at the end of 2018, the total number of bridges in service in China reached 851 500, ranking first in the world. Among these bridges, the medium and small-span concrete bridges accounted for the vast majority. Small and medium-sized concrete bridges have been in service for around 20 years, and they are in the period of emergence and development of defects. These tremendous bridges place higher demands on rapid state assessment and damage identification methods. In recent years, the influence line (IL) has been an emerging identification method, which is convenient to obtain a reliable evaluation. As a result, it has a good application prospect for the state evaluation and damage identification of medium and small-span concrete bridges (Zhang & Liu, 2019).

The bridge IL is a curve representing the whole response of a specific cross-section due to the variation of the load position (Chen, Cai, & Li, 2016). As a global index of the bridge, it contains the information of boundary conditions, geometric parameters, material composition, and other feature information of a structure. Consequently, it has been widely used in the field of model modification (Xiao, Xu, & Zhu, 2015), damage detection (Wu et al., 2016), and state assessment (Wang et al., 2017). According to the type of response, the IL can be divided into strain IL, bending moment IL (Chen et al., 2019), shear force IL (Wu, Wu, & Yang, 2019), and so on. Among these, the strain IL and displacement IL have the most widespread applications, owing to their convenience in the measurement. Chen et al. (2015) used the first derivative of the

stress IL as the index to determine the damage location and verified its applicability in long-span suspension bridges. However, the research by Alamdari et al. (2019) indicated that strain-based IL is likely to cause misjudgment of damage localization. Consequently, many scholars concentrate on the damage identification method based on displacement IL (Oskoui, Taylor, & Ansari, 2019; Zeinali & Story 2017).

It is essential, yet challenging, to acquire the actual bridge IL by measured data. Considering that the vehicle loads of the bridge are all dynamic loads, there is no practical feasibility to directly obtain the static load IL. The process of extracting static load IL components based on dynamic load IL is called quasi-static load IL identification. The quasi-static IL with the dynamic fluctuation components separated is smoother and more sensitive to changes in structural stiffness. As a result, it provides the basis for accurate damage identification. The IL identification is also called IL extraction, which means separating the static composition and filtering the noise at the same time. The IL measured form in-site load test inevitably contains noise and a vehicle-bridge dynamic effect, leading to difficulties in the accurate extraction process (Zhu & Law, 2015). Yang & Lin (2005) provided an elaborate theoretical extraction method of static and dynamic composition, laying a solid foundation for the identification of static load IL. Sun et al. (2018) separated the static component and dynamic component of displacement IL by combining the vehicle-bridge interaction effect and the finite element method. Chen et al. (2015) adopted a mathematical regularization method to identify ILs based on the in-site measurement data, while Zheng et al. (2019) proposed a regularized least-squares QR decomposition method, but its effect was verified based on numerical analysis and it lacked experimental support. Xiao, Xu, & Zhu (2015) derived the relationship between mode shape and IL to perform the identification, while this method had the limitation in a variety of dynamic property parameters. Zeinali & Story (2018) described a damage localization and quantification method based on multi-parameter Tikhonov regularization and the identified IL. However, this method requires multiple iterations and tedious calculations. According to the literature review, most of the studies mentioned above are limited to numerical simulation methods or laboratory tests, as a result, an in-depth comparison of the identification methods and field test verification are still missing.

It can be summarized that the previous works for quasi-static IL identification and damage identification have already made great breakthroughs, but some shortcomings still remain. First of all, the comparative evaluation of the identification method for quasi-static load IL is not sufficient. When vehicles cross bridges, in reality, the dynamic

load effects are inevitable. Consequently, a comprehensive evaluation and comparison of quasi-static load IL extracting methods have universal practical significance and an important engineering value. Secondly, the current damage identification and localization methods based on IL need tedious calculations and have many constraints. As a result, there is an urgent need for a rapid damage localization method based on IL. To solve the above problems, this paper mainly performs two aspects of work: the comprehensive comparison and evaluation of static load IL extraction methods and a rapid damage localization method for equal span bridges. Specifically speaking, this paper makes the following contributions:

We put forward two types of errors between the extracted quasi-static load IL and the measured IL, and for the first time, we have carefully evaluated the three methods of extracting the quasi-static load influence line. The influence of loading speed on the IL is further explored. Finally, the recommended method for extracting the quasi-static load IL is given.

We propose a two-stage rapid damage identification method for the equal-span bridge that first locates the damaged span and then locates the damage within the span. The damaged span is determined based on the ratio of the difference of IL under the same load, and the damage location is determined by the exceedance probability of the difference between multiple normalized IL and the benchmark IL. The exceeding probability method greatly reduces the accidental errors of tests and enhances their reliability. As a result, a rapid damage localization method from the whole to the local is formed. Overall, this paper completes the discussion of the key issues of the whole process based on the IL for damage identification, with special attention paid to the pre-processing of measured IL data and the efficient application of deflection IL.

1. Field test of IL

To illustrate the feature and the promising use of bridge deflection IL, a field test was conducted on a multi-span simply supported bridge located in southeast China. The entire bridge consists of a total of 5 spans, and each span has a length of 30 m. The upper structure consists of four T-beams with a height of 2.0 m, and they are connected as a whole by five transverse partitions. The bridge has been in operation for 14 years, and now some crack defects have appeared in part of the spans. The non-contact radar dynamic deflection tester IBIS equipment was used to measure the displacement IL of this bridge under the loading

of a truck in every span. The upper structure of the bridge with the measuring points and the IBIS equipment measurements are shown in Figure 1. The measurement points are located in the middle of each span along the bridge and the 2nd girder in the transverse direction. The field test was carried out in the early morning with closed traffic.

2. Measurement instrument

The IBIS equipment is a microwave interferometry-based system for remote static and dynamic monitoring. This equipment is made by IDS GeoRadar provider, a company founded in 1980 in Pisa, Italy. It has not only good applicability to conventional static load-displacement observation, but also makes continuous observation of high-frequency dynamic displacement observation possible. This equipment is suitable for bridge dynamic deflection monitoring mainly due to its outstanding technical features as follows: (1) Remote sensing. Real-time remote sensing at up to 1 km with no need for equipment to be installed on the monitored structure; (2) Accurate measurements. Measures displacements of as little as 0.01 mm within a range of 0.5 km. No standard instrument can achieve such accuracy; (3) High sampling frequency. Structural vibration sampling up to 200 Hz. Therefore, this instrument exhibits unique applicability to the dynamic deflection of the bridge during operation.

As for the loading truck, a heavy truck of relatively fewer axles is more suitable for field tests of ILs. The truck with fewer axles is conducive to clarify the position of the load, and the sufficient truck

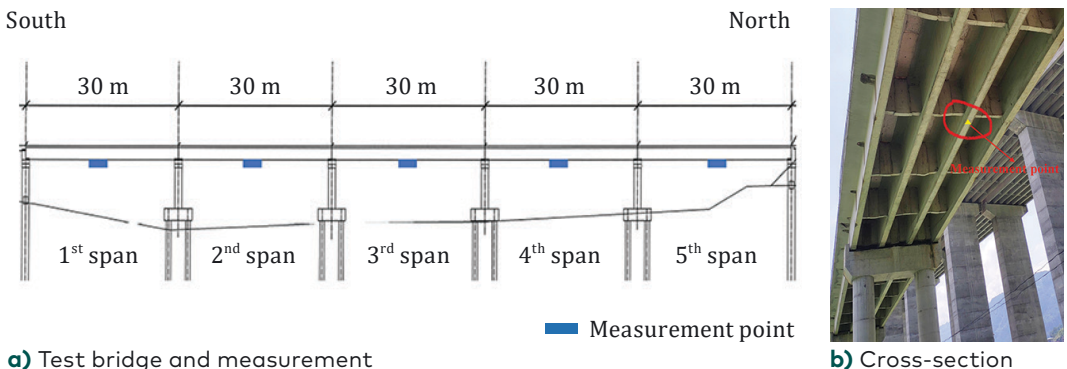


Figure 1. Layout of spans and photo of measurements in the test bridge

weight is to cause enough structural deformation response. In the field test, we selected a three-axle muck truck with a total weight of 18.4 tons as the loading vehicle. The maximum deflection of about 2 mm is produced, which can be satisfied considering the accuracy of our measuring instrument.

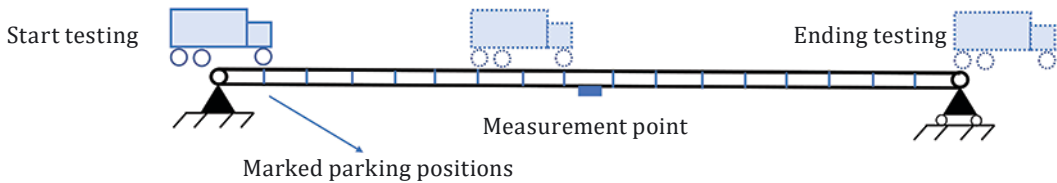


a) IBIS instrument



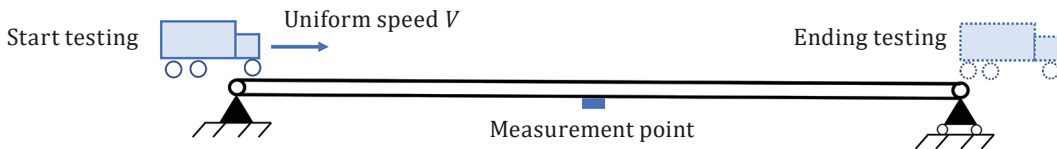
b) The loading truck

Static IL measurement



c) Static test

Dynamic IL measurement



d) Dynamic test

Figure 2. Photos of IBIS instrument and the loading truck and schematic diagram of loading conditions

3. Loading conditions

Considering the significant difference between the static and the dynamic load IL, it is of great necessity to measure the static and the dynamic load IL, respectively. The acquisition of static IL was obtained by measuring the static deflection induced by the loading truck posed in every meter in the longitudinal direction of the bridge. To refine the loading process, the markers were made for every meter on the bridge as the parking mark position. When the first axle loaded at the parking mark position, the truck was stopped, and the engine was turned off for a while to measure the static deflections. Consequently, the discrete static IL was obtained. The test started at the time when the first axle entered the bridge across and ended at the time when the third axle left the bridge. Correspondingly, the acquisition of dynamic IL was achieved by measuring the deflection time history data with the truck moving through the whole bridge at a uniform velocity. Additionally, to evaluate the influence of velocities, a set of different loading velocities were tested. The loading conditions are illustrated in Figure 2 and the velocities of the dynamic loading test are shown in Table 1.

4. Raw data

According to previous studies by Wang et al. (2017), for both a single-span beam with general boundary condition and a multi-span continuous beam, the real ILs of strain and deflection can be described by a piecewise cubic polynomial. Through the static load test, the static load

Table 1. Test load conditions

Number of load condition	Velocities, km/h	Load condition description
Load condition 1	0	Static IL acquisition: the loading truck is parked once every meter in the longitudinal direction of the bridge deck, and the deflection of the bridge at each loading position is measured as a discrete static load IL.
Load condition 2	10	Dynamic IL acquisition: during the test, the loading vehicle passes through the bridge at uniform velocities of 10~50 km/h; the same lane is used in the same loading direction.
Load condition 3	20	
Load condition 4	30	
Load condition 5	40	
Load condition 6	50	

displacements per meter along the bridge span are obtained as shown in Figure 4. The displacement of each static load test point is the result of the superposition of multiple axle concentrated forces in the elastic stage of the structure. Considering that the deflection IL is a cubic curve under the concentrated force of each axis, it is believed to be also a cubic curve after multi-axis superposition. Therefore, the static load IL of the real bridge can be obtained by applying multiple static deflections measured by cubic curve fitting, which is reflected by the red line in Figure 3.

For the dynamic IL at different load velocities, the common features are the multiple high-frequency oscillations. That is to say, the dynamic

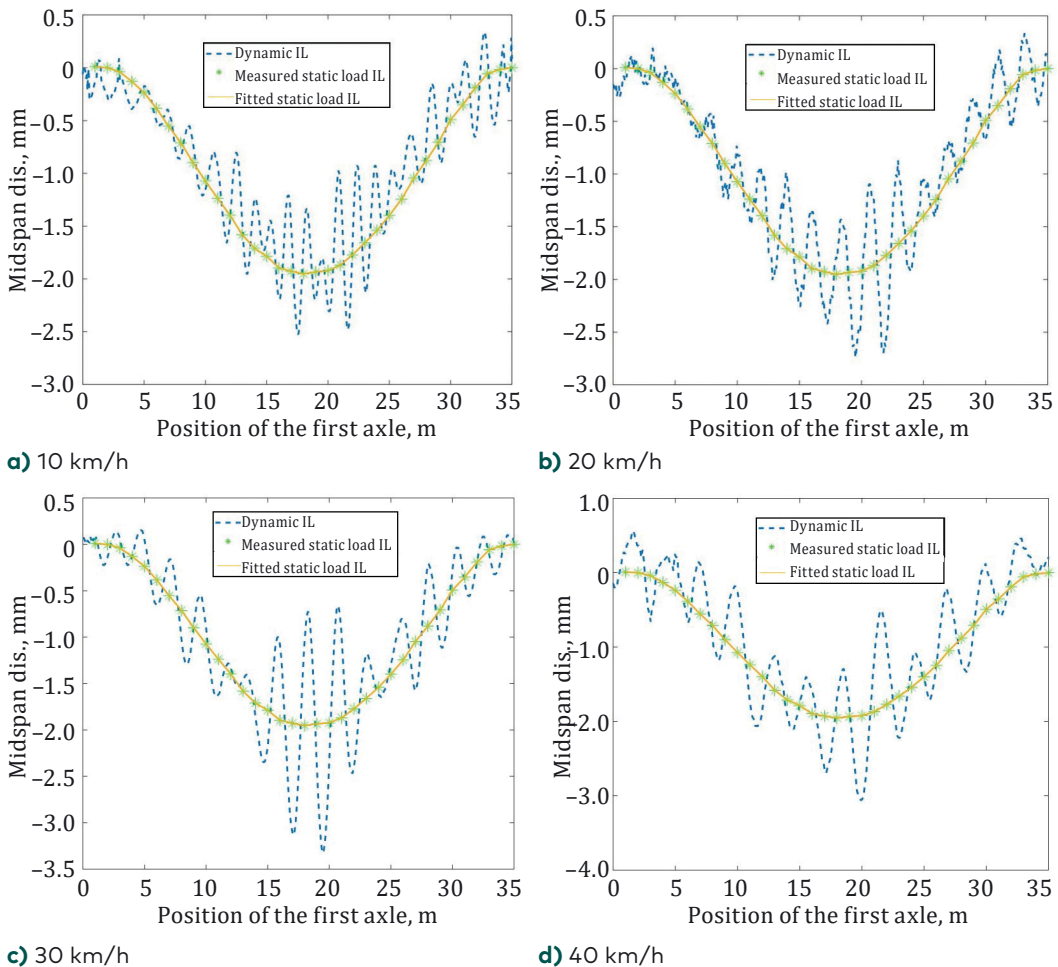


Figure 3. Raw data in the 2nd span of 4 loading conditions

IL is a kind of curve that oscillates around the static load curve. The oscillation characteristics are also noteworthy, i.e. the lower velocity dynamic ILs oscillate less in the amplitude than that of higher velocity dynamic ILs. This is because the impact of vehicles at high speeds is greater than that of low speed due to the roughness of pavement. In turn, the dynamic ILs of higher velocity tend to have relatively larger oscillation amplitudes. These oscillations have significant adverse effects on the amplitude. More importantly, they may even mask the local change of IL caused by structural damage. As a result, it is of great significance to eliminate local oscillation and restore the truest possible quasi-static load IL.

5. Quasi-static IL identification methods

As mentioned above, the key to the processing of the measured dynamic IL is to effectively eliminate the oscillation caused by the dynamic load effect. Consequently, this part focuses on the oscillation elimination method based on signal processing methods. To obtain a more accurate identification method, two kinds of error indicators are first proposed. Then, the effectiveness of the three methods is evaluated. At last, a recommended method is given and the key parameters of this method are discussed.

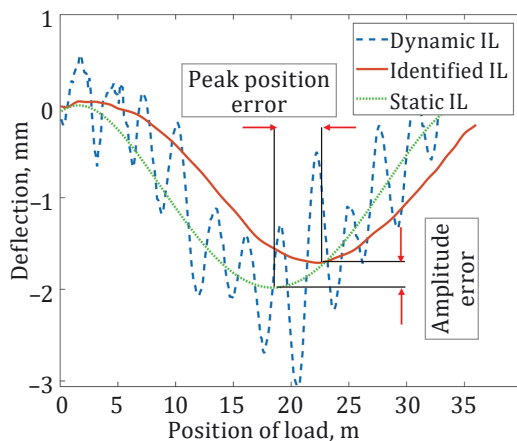


Figure 4. Two kinds of errors: amplitude error and peak position error

6. Two kinds of errors and the error indicators

6.1. Two kinds of errors

Through the extensive observation and comparison of the identified IL and the static load IL, two types of errors are found commonly in many recognition methods. As shown in Figure 4, the first kind of error is an amplitude error, which refers to the difference of maximum value between the identified IL and the static load IL. This kind of amplitude deviation directly affects the judgment of the occurrence of damage. The other kind of error is the location bias of the maximum value, which leads to the discrimination of the damage localization by offsetting the overall position.

6.2. Error indicators

To quantitatively describe the accuracy of the identified IL, two indices are put forward for the two kinds of errors, respectively. Specifically, E_1 represents the extent of amplitude error, with the ability to eliminate the absolute effect of the difference by a normalization method. Correspondingly, E_2 describes the magnitude of the second type of error. The specific calculation process of the indicator is as follows:

1. amplitude error

$$E_1 = \frac{1}{M} \sum_{i=1}^M \left| \frac{IL_{id}(i) - IL_s(i)}{IL_s(i)} \right|, \quad (1)$$

where M represents the total number of data points; $IL_{id}(i)$ and $IL_s(i)$ represent the identified IL and static load IL, respectively.

2. peak position error

$$E_2 = \left| \frac{L_{id} - L_s}{L} \right|, \quad (2)$$

where L represents the length of the measured span, L_{id} and L_s represent the peak position of the identified IL and the static IL, respectively.

7. Comparison among different methods

Three digital signal processing methods were performed to deal with the problem of the dynamic load effect of the measured dynamic IL. The methods included the finite impulse response filtering (FIR), the empirical mode decomposition (EMD), and the Daubechies N wavelet (dbN). As a classical kind of digital filter, the FIR method is

often adopted to modify or change the characteristics of signals in the time or frequency domain. Park et al. (2013) obtained the FIR method in a wireless displacement measurement system using acceleration responses, and Ding, Zhao, & Li (2017) implemented the FIR method in the strain IL separation of a steel-truss arch railway bridge. The EMD is firstly proposed by Huang et al. (1998), which is suitable for nonstationary data. Xia et al. (2017) used this method to achieve the goal of separation of temperature-induced strain in a suspension bridge. It can also be used for bridge damage detection owing to the ability to decompose a single. The wavelet analysis has become a common way of decomposing a signal in the frequency-time domain. Yang et al. (2019)

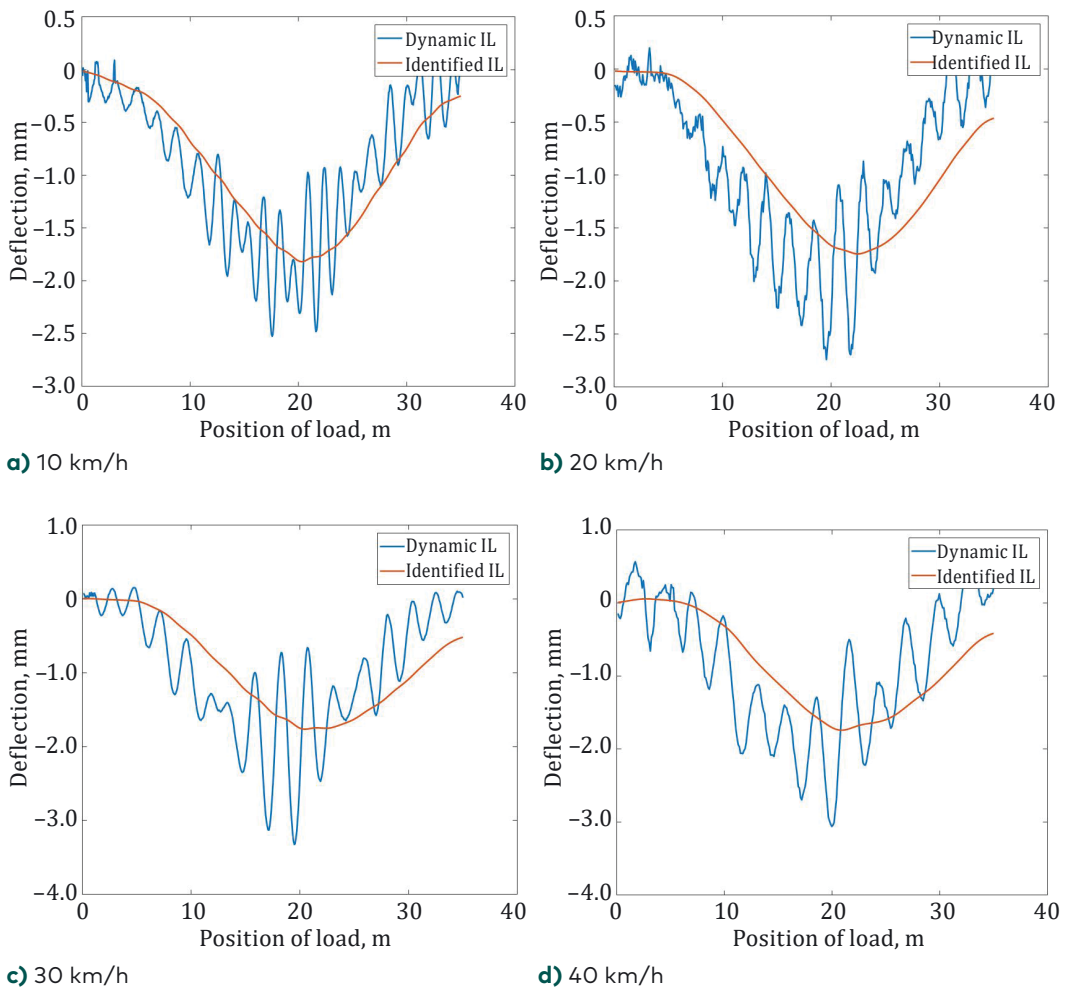


Figure 5. Identified results of the FIR method

performed a wavelet decomposition in the temperature-induced strain extraction. As for the Daubechies N wavelet, it is a handy and typical wavelet, where N is the vanishing moment. Consequently, it is called the dbN method. All the above three methods fit the separation of the overall trend in non-stationary data; besides, they are easy to operate. Thus, they are chosen to conduct the quasi-static IL identification.

To evaluate the effectiveness of these methods, the sensitivity of two types of errors of the methods under various velocities was assessed. Specifically, in the dynamic load test, the dynamic IL test was repeated 5 times at each velocity, so that the accidental errors could be eliminated.

7.1. The FIR method

It can be seen from Figure 5 that the FIR method can achieve the goal of quasi-static IL by significantly eliminating dynamic load effects. However, its effectiveness at different velocities is different. Specifically, the identified curves become smoother as the test velocities increase, while the effectiveness of maximum amplitude and position declines. This trend is more intuitively demonstrated in Figure 6. Both two kinds of errors increase significantly with velocity. Moreover, both the correlation coefficient of two errors and velocity is bigger than 0.88, which indicates that with the increase of velocity the applicability of this method declines. In summary, the FIR method has the capacity of quasi-static IL identification, but the correlation of errors and velocities limits its application in high-velocity load conditions. The FIR method here uses low-pass filtering. First, the original signal is analyzed by the frequency

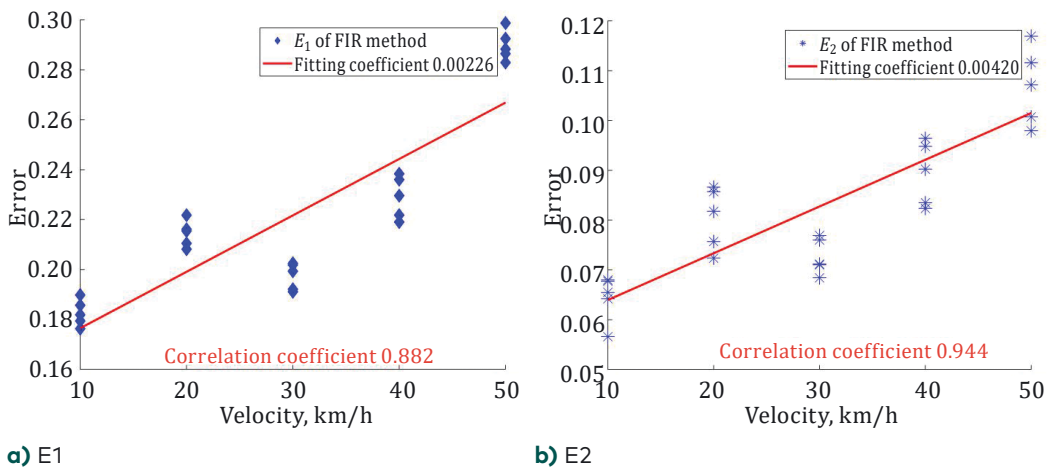


Figure 6. Error analysis of the FIR method

spectrum, the frequency range of the vehicle-induced response is determined, and then the corresponding filtering order and cutoff frequency are set. With the increase of the filtering order, the filtered signal has phase distortion and the output signal lags behind the input signal, resulting in a non-zero phenomenon on the right side, which is an inherent defect of this method.

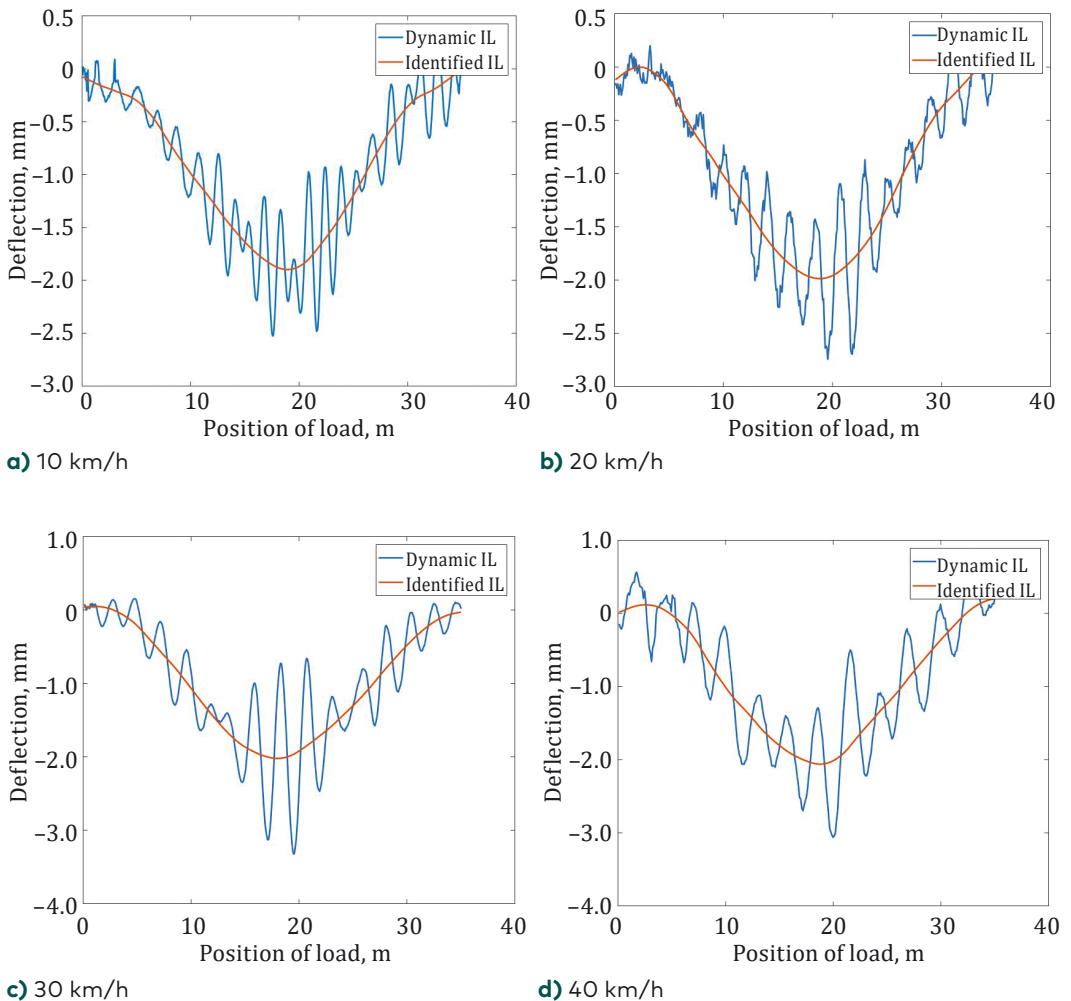


Figure 7. Identified results of the EMD method

7.2. The EMD method

It can be seen from Figure 7 that the EMD method can achieve a better result by giving out a smoother quasi-static IL. As to the velocity, it can be seen from Figure 8 that for the EMD method only the first kind of error is related to velocity. This means with the increment in velocity, the identification result of the maximum is not affected by the loading velocity. Meanwhile, the amplitude of the maximum value is still influenced by the load velocity, leading to an imperfect performance in high velocity. As a result, in terms of the accurate error analysis, the EMD method is still not perfect.

7.3. The Daubechies wavelet method

From Figure 9, it is obvious that the ILs identified by the dbN method have hardly significant deviations in various velocities, which indicates the DBN method can obtain a relatively better result. Both of the two kinds of errors of this method are relatively small. The DBN wavelet has a better regularity, i.e. the smooth error introduced by the wavelet as a sparse basis cannot be easily detected, making the signal reconstruction process smooth. Furthermore, the nature of these errors of the DBN method does not change with the velocity, which can be seen from the weak correlation in errors and velocities in Figure 10. This feature indicates that the DBN method applies to quasi-static load IL identification under a load of various velocities.

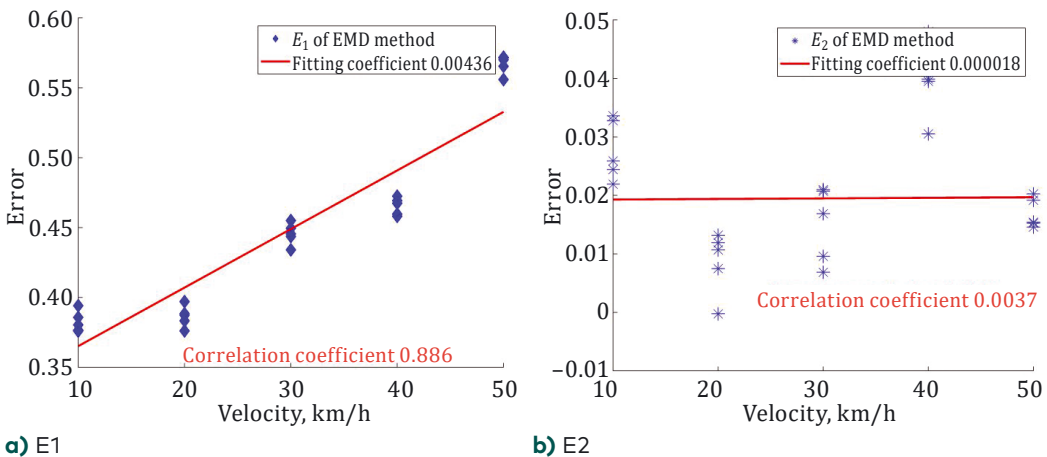


Figure 8. Error analysis of EMD method

In summary, the three commonly used identification methods can achieve the purpose of removing the dynamic load composition and filtering out the noise. The averaged error indicators E1 of the three methods are: 0.23, 0.47, and 0.06, respectively. The corresponding error indicators E2 of the three methods are 0.08, 0.01, and 0.02. Among the three methods, the FIR method may have an offset of the position of the signal extreme value, causing interference to the damage localization. The EMD method is relatively inaccurate in the identification of extreme amplitudes. Comprehensively, wavelet decomposition, with the wavelet

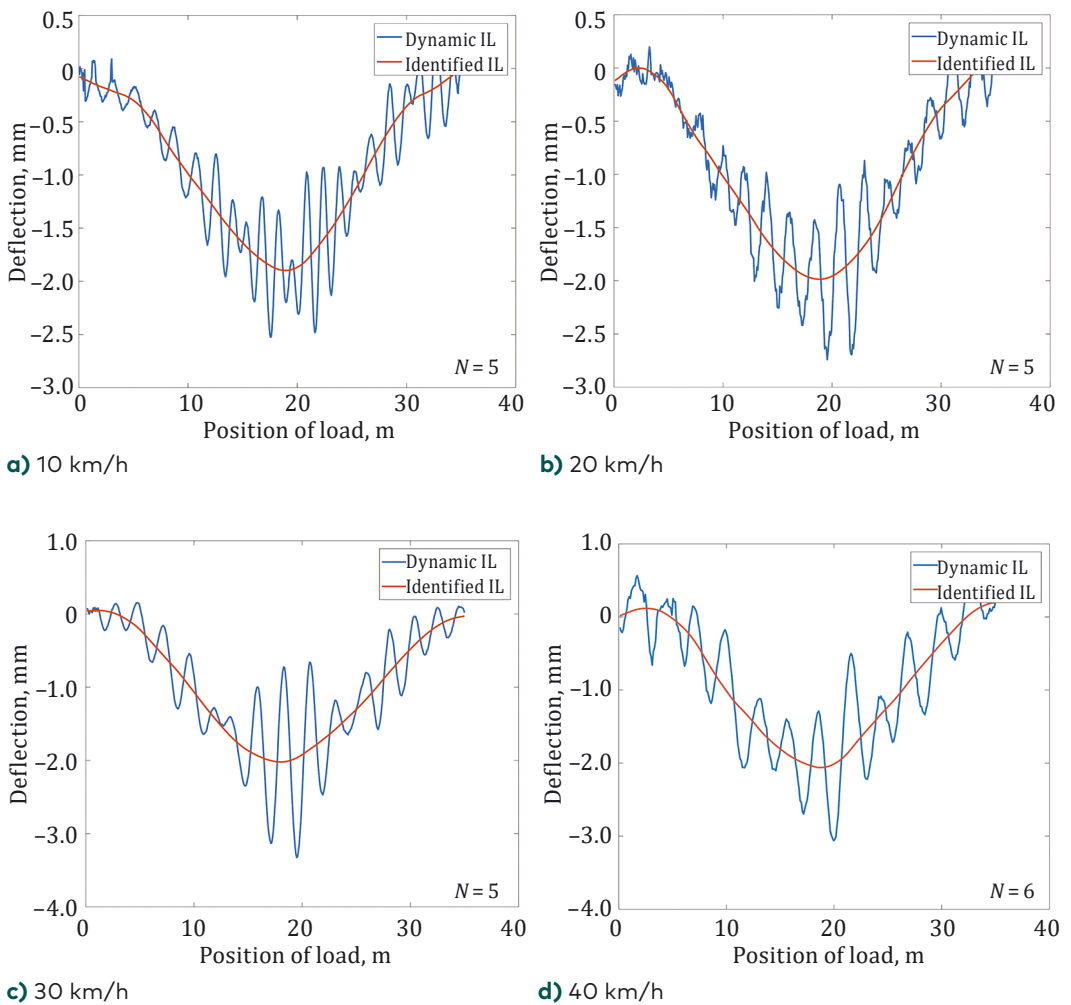


Figure 9. Identified results of the dbN method

basis of the dbN wavelet method, is the most accurate in terms of the proximity of the amplitude and the position of the amplitude after the identification. As a result, it is recommended as the desired quasi-static load IL recognition method.

The applicability of the signal processing method for the static load IL identification mainly has two requirements: 1) to eliminate the fluctuation of the dynamic load effect and restore the true amplitude and curve characteristics; 2) to retain the local characteristics of the IL caused by structural damage. The dbN method can meet the above requirements. Specifically, the N of the dbN wavelet represents the vanishing moment. From the perspective of signal processing, the larger the vanishing moment and the longer the support length, the smaller the coefficient of the high-frequency component after signal reconstruction, thereby the high-frequency unfavourable component of the coupled vehicle bridge vibration in the dynamic load test is eliminated. In terms of signal form, the data are smoother and show the overall trend characteristics.

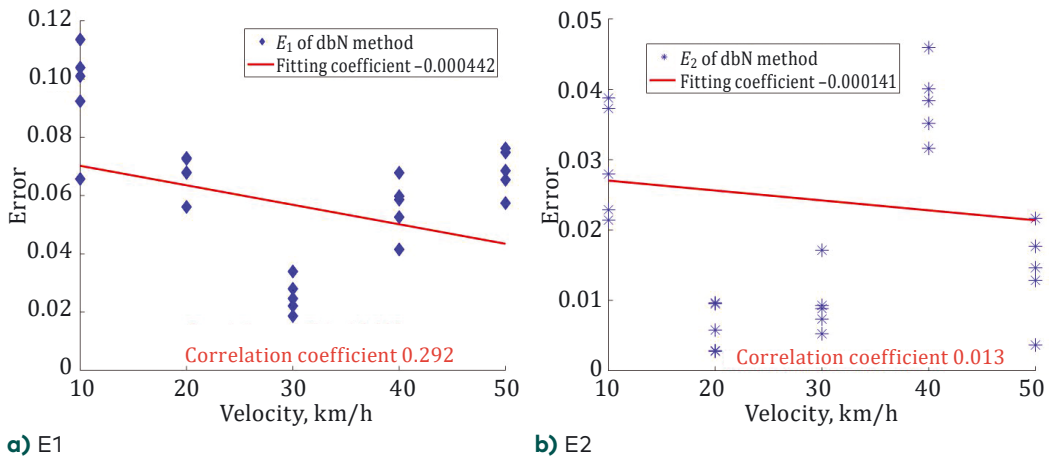


Figure 10. Error analysis of the dbN method

8. Determination of N of the dbN method

As for Daubechies N wavelet, the most critical issue is determining N vanishing moment. The characteristic of the dbN wavelet is that as the order (sequence N) increases, the order of the vanishing moment increases, and the higher the vanishing moment, the better the smoothness, the stronger the localization ability in the frequency domain, and the better the frequency band division effect. However, it will reduce the tight support in the time domain, at the same time, the number of calculations will increase greatly resulting in reduced real-time performance.

To explore the determination of the vanishing moment N in the dbN method, different values of N are used for the identification of the measured dynamic load IL, as plotted in Figure 11. It is clear that as the vanishing moment increases, the curve becomes smoother. When the value of N is about 6, the recognition achieves better results. When N is greater than 7, the deviation of the recognition curve becomes significantly larger.

To further explore the suitable value of vanishing moment N in different loading velocities, the two kinds of errors are calculated and shown in Figure 12. At the same velocities, two types of indicators first decrease and then increase as N increases. At the same N , two types of indicators first decrease and then increase as N increases. Based on this trend, the most suitable N can be determined. The appropriate values of

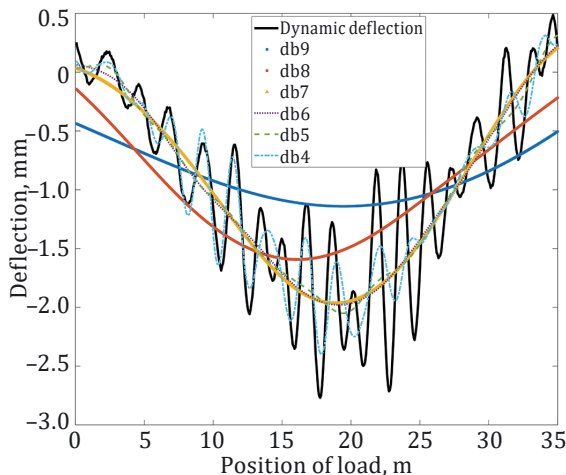


Figure 11. Identified results with dbN method using different N

N are concentrated between 5 and 7. Through calculation and analysis of all measured data, the appropriate recommended values of N are shown in Table 2.

Table 2. Recommended of N of dbN Method

Velocity	≤ 20 km/h	20~40 km/h	≥ 40 km/h
N of dbN	5	6	7

9. The two-stage damage localization method

The identification of the unit-force IL from measured IL of multi-axle loading is of great need for the long-term automatic bridge IL monitoring. If the unit-force IL can be identified from the random traffic flow of the operational load, the bridge evaluation application based on the IL will be greatly promoted. However, due to the sparseness of the vehicle's position matrix, the matrix singularity is easily caused, which makes it difficult to solve the unit-force IL extraction problem (Frøseth et al., 2017).

To avoid the above difficulties, this paper proposes a two-stage identification method for equal-span simply supported beam bridges. The difference between the IL of adjacent spans is used as the index for the judgment of the damaged span, thus avoiding the problem of

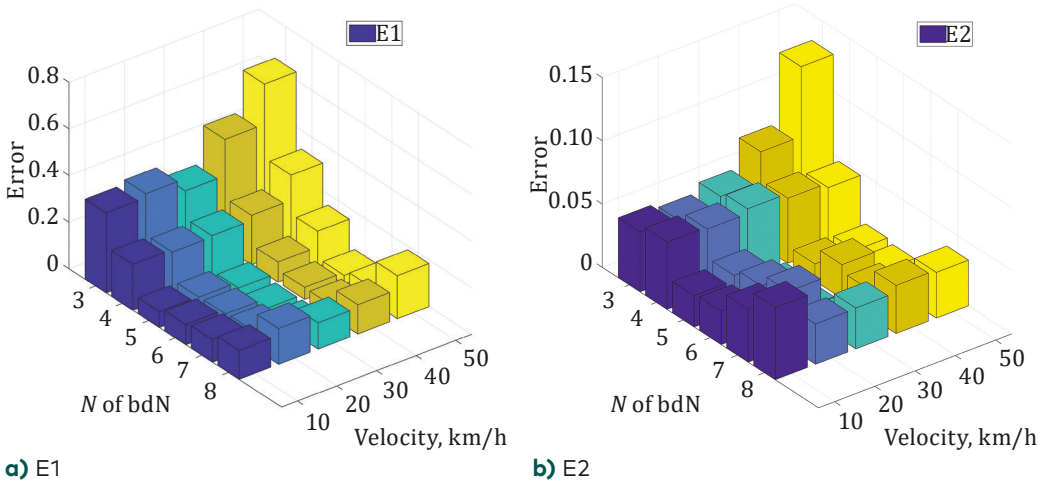


Figure 12. Errors with different velocities and N

solving the unit-force IL. Eventually, the rapid discrimination of the damaged span and the local damage can be achieved. The equal-span simply supported beam bridges are prevalent in small and medium span bridges, especially on low-grade highways and high-speed railways. Our method is strictly applicable to equal-span simply supported beams.

10. Framework of the two-stage damage localization

The equal-span simply supported beam bridges are commonly used in the small and medium span bridges. Based on the hypothesis that equal-span bridges should have the same response under the same load, a two-stage damage localization method is proposed. The damaged span is first determined according to the amplitude ratio of the response data, and then the damage position is determined according to the influence derivative of the IL. Thereby, the rapid localization of the damage based on the IL is implemented. The basic flow of this method is shown in Figure 13.

Firstly, the dynamic ILs of the full bridge in all the spans were measured, respectively. To improve the reliability of the measurement results, multiple ILs were obtained using the same vehicle in multiple reciprocal movements over the full bridge at different speeds. Then the dbN wavelet method was applied to identification of the quasi-static load IL of each dynamic IL. After that, the similarity indices of adjacent spans were calculated. Subsequently, the damaged span was determined by the mean similar indicators of different velocities. Considering that the theoretical static load IL was a third-order parabola, the benchmark IL of each span could be obtained by fitting the average amplitude of each span. The second stage was the localization of the local damage within the span. To achieve this goal, the IL at multiple velocities was homogenized, and then the derivative of the normalized IL and the normalized benchmark IL at each velocity were calculated. Then the derivative threshold was set up to calculate the exceedance probability of multiple ILs. Finally, the exceedance probabilities were converted into the unit damage probability per unit along the span direction, which was used as the basis for local damage judgment. Thereby, the determination of the damage position within the span was implemented.

10.1. Stage 1: Damaged span identification

The specific steps of the method for fast damage identification and localization of equal-span bridges are as follows. Firstly, the deflection IL of each span at velocities of 10 km/h, 20 km/h, 30 km/h, 40 km/h, and

50 km/h are obtained, respectively. It should be repeated five times at each velocity to get enough data. Then the dbN wavelet decomposition method is adopted to identify quasi-static load IL. The total number of spans in the whole bridge is assumed as z , so the corresponding quasi-static IL signals of the first span to the z -th span are respectively recorded as $Y_{q1}(t), Y_{q2}(t), \dots$ and $Y_{qz}(t)$.

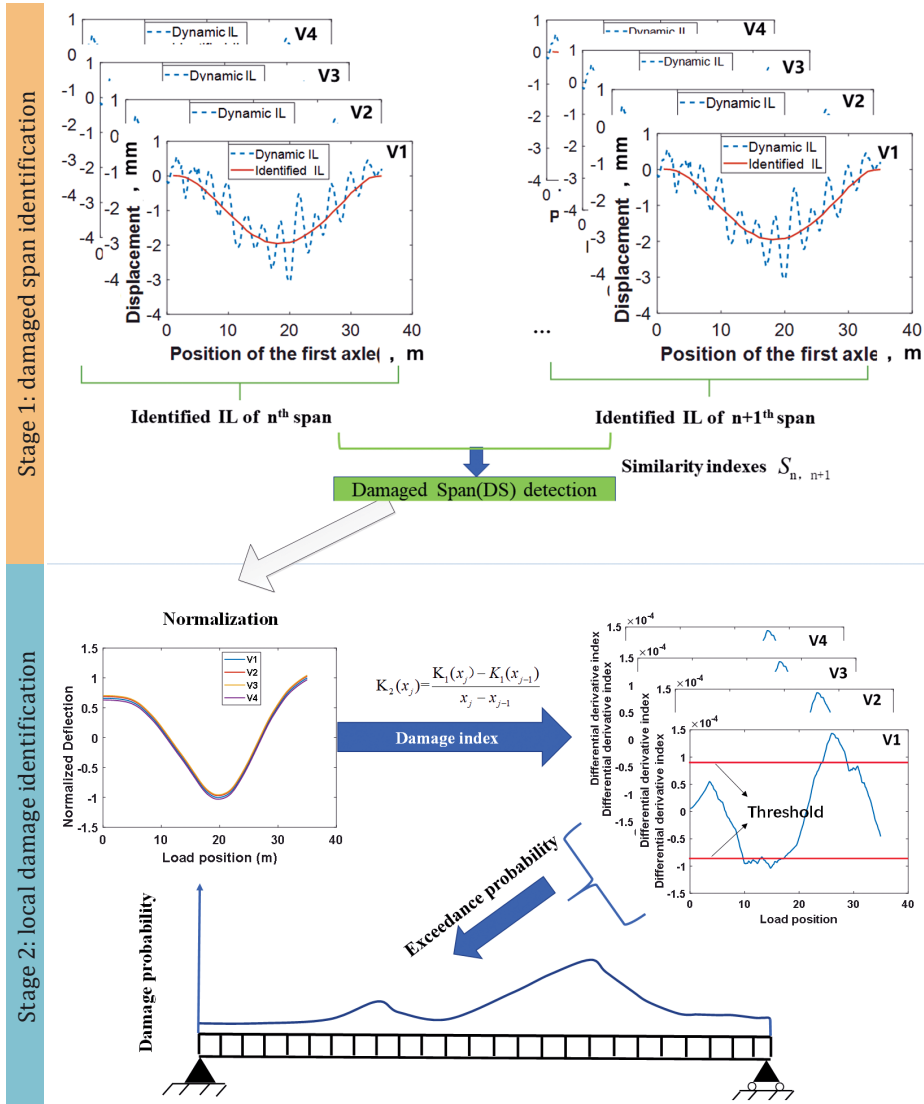


Figure 13. Flow chart of the two-stage damage identification method

Based on this, the similarity indices can be calculated as follows:

$$S_{n,n+1} = \frac{1}{T} \sum_{j=1}^T \frac{Y_{qn(j)}}{Y_{qn+1(j)}}, \quad (3)$$

where $S_{n,n+1}$ is the similarity indices of n -th span and $n+1$ -th span. $Y_{qn(j)}$ is the value of quasi-static load IL of n -th span at the time of j . Similarly, $Y_{qn+1(j)}$ represents the value of $n+1$ -th span at the corresponding time. And T is the total number of the data points, also the total number of the time series of IL. At last, the damaged span can be identified according to Table 3. The criterion of the index is based on the results of many real bridge condition assessments, regarding Chinese bridge condition assessment codes. Moreover, to enhance the accuracy of the threshold, the verification of numerical finite element simulation was carried out.

10.2. Stage 2: Local damage localization

First, it is necessary to calculate the IL difference between damaged span and benchmark IL. Then, it is necessary to normalize the identified quasi-static load IL at multiple velocities to eliminate the difference in amplitude that may be caused by different velocities. Thereby, comparison and calculation of measured IL can be achieved. Normalizing the damaged span static-load IL takes place by

$$Y_n(x_i) = \frac{Y_{qd}(x_i)}{|\max Y_{qd}(x)|}, \quad (4)$$

where $Y_q(x_i)$ is the normalized quasi-static load IL of the damaged span, $Y_{qd}(x)$ is the quasi-static load IL of the damaged span, and x_i is the load position. The benchmark IL is determined by the IL of undamaged spans. Accordingly, the normalized benchmark IL can be obtained by

$$Y_{nb}(x_i) = \frac{Y_{qb}(x_i)}{|\max Y_{qb}(x)|}, \quad (5)$$

Table 3. Basis of damaged span identification

Similarity indices	Identification of results	Result description
$S_{n, n+1} > 0.8$ and $S_{n+1, n+2} < 1.25$	No obvious degradation	The situation of all spans is similar
$S_{n, n+1} \leq 0.8$ and $S_{n+1, n+2} \geq 1.25$	$N+1$ -th span is damaged	Individual discrete span has a significant decline
$S_{n, n+1} \leq 0.8$ and $1 < S_{n+1, n+2} < 1.25$ and $S_{n+2, n+3} > 1.25$	$N+1$ -th and $N+2$ -th span may be damaged	Significant reduction in two or more consecutive spans

where $Y_{qb}(x)$ is the benchmark IL, which is a fitted cubic parabola combined with the amplitude of the identified static IL. The 'benchmark' here mainly means that the fitted IL is the IL of the theoretical intact structure, and there is no local fluctuation of the curve caused by local damage.

The difference of quasi-static load IL and benchmark IL is calculated by

$$K_1(x_i) = Y_n(x_i) - Y_{nb}(x_i). \quad (6)$$

This difference contains the oscillations caused by local damage, which is the basis for damage localization. Whereas, the value of this value is relatively small and difficult to judge. Tan, Lu, and Liu (2018) proposed a damage localization method based on displacement IL difference and its derivatives. Inspired by this method, the first derivative of the IL difference is proposed to describe the rate of change of the difference, which can magnify the difference of the local stiffness variation induced by local damage. The damage indicator is defined by the rate of change of the difference as follows:

$$K_2(x_j) = \frac{K_1(x_j) - K_1(x_{j-1})}{x_j - x_{j-1}}. \quad (7)$$

Finally, to clearly mark the potential localization of the damage, a method based on the exceedance probability of IL is proposed. For each IL, it is necessary to divide it into segments of 1 meter in length and calculate whether K_2 within the segment exceeds the threshold. If more than half of the points in the segment exceed the threshold, the segment is determined as a damaged segment. Then the proportion of the damaged segment is calculated to obtain the probability of damage in each section. The threshold value is obtained by the change of K_2 caused by the stiffness reduction by 10% of the unit section using the finite element simulation. In order to eliminate accidental errors, the number of ILs for independent measurement should be no less than 25 and include various loading speeds.

11. Verification

11.1. Application of the two-stage identification method

The bridge used for experimental verification is the same bridge used for IL collected in the second part of the article. The information about the bridge is not repeated here. Firstly, the discrimination of the first stage for the identification of damage span is performed. The

adjacent cross-similarity index is calculated by the quasi-static IL signal to determine the damaged span. The adjacent-span similarity index is calculated by Equation (1). It can be seen from Table 4 that the similarity index of span 1–2 and that of span 2–3 are far from the normal value. Moreover, the similarity index of span 1–2 is less than the lower limit, and the span 2–3 is greater than the upper limit. Based on this finding, the second span is identified as the damaged span.

Table 4. Similarity indices of the test bridge

Location	Span 1–2	Span 2–3	Span 3–4	Span 4–5
Similarity indices	0.76	1.38	1.03	0.96

Then the second stage of damage is performed to locate the local damage within the damaged span. The difference derivative index is calculated by Equations (6) and (7). To enhance the credibility of the results, all the measured IL data are used to calculate the difference derivative, then according to the threshold, the exceedance probability can be obtained as shown in Figure 14. It is finally determined that the damage positions are 11 m, 14–15 m, and 23–25 m of the second span.

11.2. Verification of the method

The results of the visual inspection of the bridge in 2019 showed that the second span had obvious technical state decline. The number of bridge defects was relatively higher than in the other spans. This confirms the correctness of the damaged span identification results.

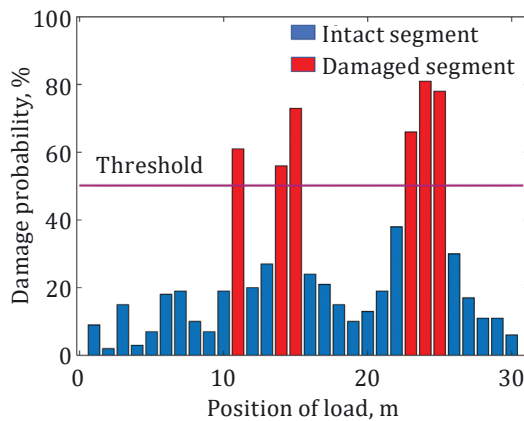


Figure 14. Damage probability along span direction

Through the visual inspection of the actual bridge, it was found that there were many cracks in the second span. The upper load-bearing member was inspected and the spalling was found at the concrete web, with a total area of 0.26 m^2 , located at 4 m and 14 m along the longitudinal direction. Eight types of concrete breakage were identified in the girder roof with a total area of 0.47 m^2 , located at 12 m, 16 m, and 23 m along the span. What is more, 173 vertical cracks were found on the web, total length was 148.7 m, and none of them exceeded the limit criterion, distributed at 15 m, 17 m, and 22 m. Besides, 8 U-shaped through cracks were found with a total length of 25.9 m, distributed around 17 m. The three main types of damage and a schematic diagram of their locations are shown in Figure 15.

It can be seen from Figure 15 that the damaged span and span damage position of the bridge agree well with the result derived from the two-stage identification method proposed in this paper. The application of the two-stage damage identification and localization method based on the IL can quickly determine the damaged span and the damage location. Furthermore, the actual detection of the defect distribution and the determination of the identified damage area are consistent, so that the applicability of the method is verified.

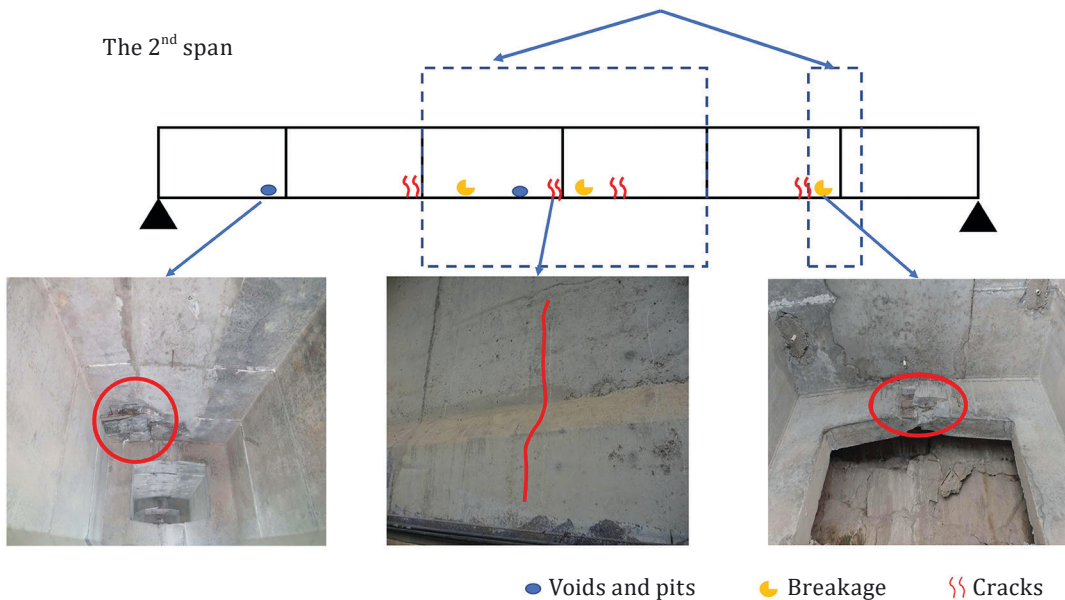


Figure 15. Identified damage location and detected damage distribution

Conclusions

Firstly, the quasi-static IL identification method focusing on field measurement has been studied in the paper. The identification method proposed in the paper requires multiple ILs obtained using the same vehicle crossing the bridge multiple times. However, it is worth noting that by means of data normalization and signal processing such as dbN, the method proposed in the paper can eliminate the differences caused by different speeds and achieve accurate IL identification at the engineering application level. Thus, no vehicle weighing system is required and the extraction of the IL can be achieved. Subsequently, with the identification method, a fast damage localization method suitable for equal-span simply supported beam bridges is proposed to circumvent the difficulty of unit load IL inverse solution. This method has a two-stage identification process: determination of the damaged span and the damage location within the span. A significant advantage of this method is that it achieves the goal of fast and effective positioning of bridge damage. Combined with visual inspection results, the reliability and robustness of the method are verified. The main conclusions are as follows:

1. Two kinds of errors are firstly defined between identification IL and static load IL, which can be useful indicators to quantify the effectiveness of the identification method.
2. All the dbN, FIR, and EMD methods can achieve the aim of static IL identification. Comprehensively, the wavelet decomposition method is better for identifying the peak value and position of the extremum.
3. The effectiveness of the dbN wavelet method for static load identification is influenced by the selection of N . Furthermore, the selection of N and loading velocities is relevant. Generally, N ranges 5–7, and the higher the velocities, the N value should be larger.
4. Generally, bridges with equal span lengths have the same material composition and geometry. This laid the foundation for a two-stage rapid identification method. The first stage of damaged span identification is determined by the similarity index of the IL of adjacent spans, and then the second stage of local damage within the span is determined based on the first derivative of the difference between identified IL and benchmark IL.

This study contributes to the rapid damage identification of equal-span simply supported beam bridges based on IL. Current studies have not specified the identification method of quasi-static load IL, which is of great importance in IL extraction from operation load. The results of this

study show that the dbN method is a better method with the robustness of various velocities. Based on the identified IL, the two-stage damage identification and localization method are further put forward. The method is suitable for the equal-span simply supported bridges, which has been demonstrated in this paper through fast damage identification using IL extracted from moving vehicle load.

Acknowledgments

The authors sincerely acknowledge financial support from the Fund for Distinguished Young Scientists of Jiangsu Province (Grant. BK20190013) and the National Natural Science Foundation of China (Grants. 51978154 and 51608258).

Declaration of conflicting interests

The author(s) declared no potential conflicts of interest with respect to the research, authorship, and/or publication of this article.

REFERENCES

- Alamdari, M. M., Ge, L., Kildashti, K., Zhou, Y., Harvey, B., & Du, Z. (2019). Non-contact structural health monitoring of a cable-stayed bridge: case study. *Structure and Infrastructure Engineering*, 15(8), 1119–1136. <https://doi.org/10.1080/15732479.2019.1609529>
- Chen, Z. W., Cai, Q. L., & Li, J. (2016). Stress influence line identification of long suspension bridges installed with structural health monitoring systems. *International Journal of Structural Stability and Dynamics*, 16(04), Article 1640023. <https://doi.org/10.1142/S021945541640023X>
- Chen, Z. W., Zhu, S., Xu, Y. L., Li, Q., & Cai, Q. L. (2015). Damage detection in long suspension bridges using stress influence lines. *Journal of Bridge Engineering*, 20(3), Article 05014013. [https://doi.org/10.1061/\(ASCE\)BE.1943-5592.0000681](https://doi.org/10.1061/(ASCE)BE.1943-5592.0000681)
- Chen, Z., Yang, W., Li, J., Yi, T., Wu, J., & Wang, D. (2019). Bridge influence line identification based on adaptive B-spline basis dictionary and sparse regularization. *Structural Control and Health Monitoring*, 26(6), Article e2355. <https://doi.org/10.1002/stc.2355>
- Ding, Y. L., Zhao, H.-W., & Li, A.-Q. (2017). Temperature effects on strain influence lines and dynamic load factors in a steel-truss arch railway bridge using adaptive FIR filtering. *Journal of Performance of Constructed Facilities*, 31(4), Article 04017024. [https://doi.org/10.1061/\(ASCE\)CF.1943-5509.0001026](https://doi.org/10.1061/(ASCE)CF.1943-5509.0001026)

- Frøseth, G. T., Rønnquist, A., Cantero, D., & Øiseth, O. (2017). Influence line extraction by deconvolution in the frequency domain. *Computers & Structures*, 189, 21–30. <https://doi.org/10.1016/j.compstruc.2017.04.014>
- Huang, N. E., Shen, Z., Long, S. R., Wu, M. C., Shih, H. H., Zheng, Q., & Liu, H. H. (1998). The empirical mode decomposition and the Hilbert spectrum for nonlinear and non-stationary time series analysis. *Proceedings of the Royal Society of London. Series A: mathematical, physical and engineering sciences*, 454(1971), 903–995. <https://doi.org/10.1098/rspa.1998.0193>
- Liu, H., Wang, X., Jiao, Y., He, X., & Wang, B. (2016). Condition evaluation for existing reinforced concrete bridge superstructure using fuzzy clustering improved by particle swarm optimisation. *Structure and Infrastructure Engineering*, 13(7), 955–965. <https://doi.org/10.1080/15732479.2016.1227854>
- Oskoui, E. A., Taylor, T., & Ansari, F. (2019). Method and monitoring approach for distributed detection of damage in multi-span continuous bridges. *Engineering Structures*, 189, 385–395. <https://doi.org/10.1016/j.engstruct.2019.02.037>
- Park, J. W., Sim, S. H., Jung, H. J., & Spencer, B. F., Jr. (2013). Development of a wireless displacement measurement system using acceleration responses. *Sensors*, 13(7), 8377–8392. <https://doi.org/10.3390/s130708377>
- Sun, Z., Nagayama, T., Nishio, M., & Fujino, Y. (2018). Investigation on a curvature-based damage detection method using displacement under moving vehicle. *Structural Control and Health Monitoring*, 25(1), Article e2044. <https://doi.org/10.1002/stc.2044>
- Sun, Z., Nagayama, T., Su, D., & Fujino, Y. (2016). A damage detection algorithm utilizing dynamic displacement of bridge under moving vehicle. *Journal of Sound and Vibration*, 2016, Article 8454567. <https://doi.org/10.1155/2016/8454567>
- Tan, D., Lu, Z. R., & Liu, J. K. (2018). A two-step method for damage identification in beam structures based on influence line difference and acceleration data. *Advances in Mechanical Engineering*, 10(7), 1–19. <https://doi.org/10.1177/1687814018787404>
- Wang, N.-B., He, L.-X., Ren, W.-X., & Huang, T.L. (2017). Extraction of influence line through a fitting method from bridge dynamic response induced by a passing vehicle. *Engineering Structures*, 151, 648–664. <https://doi.org/10.1016/j.engstruct.2017.06.067>
- Wu, B., Wu, G., Yang, C., & He, Y. (2016). Damage identification and bearing capacity evaluation of bridges based on distributed long-gauge strain envelope line under moving vehicle loads. *Journal of Intelligent Material Systems and Structures*, 27(17), 2344–2358. <https://doi.org/10.1177/1045389X16629571>
- Wu, B., Wu, G., & Yang, C. (2019). Parametric study of a rapid bridge assessment method using distributed macro-strain influence envelope line. *Mechanical Systems and Signal Processing*, 120, 642–663. <https://doi.org/10.1016/j.ymssp.2018.10.039>

- Xia, Q., Cheng, Y. Y., Zhang, J., & Zhu, F. Q. (2017). In-service condition assessment of a long-span suspension bridge using temperature-induced strain data. *Journal of Bridge Engineering*, 22(3), Article 04016124. [https://doi.org/10.1061/\(ASCE\)BE.1943-5592.0001003](https://doi.org/10.1061/(ASCE)BE.1943-5592.0001003)
- Xiao, X., Xu, Y. L., & Zhu, Q. (2015). Multiscale modeling and model updating of a cable-stayed bridge. II: model updating using modal frequencies and influence lines. *Journal of Bridge Engineering*, 20(10), Article 04014113. [https://doi.org/10.1061/\(ASCE\)BE.1943-5592.0000723](https://doi.org/10.1061/(ASCE)BE.1943-5592.0000723)
- Yang, K., Ding, Y., Sun, P., Zhao, H., & Geng, F. (2019). Modeling of temperature time-lag effect for concrete box-girder bridges. *Applied Sciences-Basel*, 9(16), Article 3255. <https://doi.org/10.3390/app9163255>
- Yang, Y. B., & Lin, C. W. (2005). Vehicle-bridge interaction dynamics and potential applications. *Journal of Sound and Vibration*, 284(1-2), 205-226. <https://doi.org/10.1016/j.jsv.2004.06.032>
- Zeinali, Y., & Story, B. A. (2018). Impairment localization and quantification using noisy static deformation influence lines and Iterative Multi-parameter Tikhonov Regularization. *Mechanical Systems and Signal Processing*, 109, 399-419. <https://doi.org/10.1016/j.ymsp.2018.02.036>
- Zeinali, Y., & Story, B. (2017). Framework for flexural rigidity estimation in Euler-Bernoulli beams using deformation influence lines. *Infrastructures*, 2(4), 23, Article 2040023. <https://doi.org/10.3390/infrastructures2040023>
- Zhang, S., & Liu, Y. (2019). Damage detection in beam bridges using quasi-static displacement influence lines. *Applied Sciences*, 9(9), Article 180. <https://doi.org/10.3390/app9010180>
- Zhao, H. W., Ding, Y. L., Li, A.Q., Ren, Z. Z., & Yang, K. (2019). Live-load strain evaluation of the prestressed concrete box-girder bridge using deep learning and clustering. *Structural Health Monitoring*, 19(4), 1051-1063. <https://doi.org/10.1177/1475921719875630>
- Zhao, H. W., Ding, Y. L., Nagarajaiah, S., & Li, A. Q. (2019). Behavior analysis and early warning of girder deflections of a steel-truss arch railway bridge under the effects of temperature and trains: Case study. *Journal of Bridge Engineering*, 24(1), Article 05018013. [https://doi.org/10.1061/\(ASCE\)BE.1943-5592.0001327](https://doi.org/10.1061/(ASCE)BE.1943-5592.0001327)
- Zheng, X., Yang, D. H., Yi, T. H., Li, H. N., & Chen, Z. W. (2019). Bridge influence line identification based on regularized Least-Squares QR decomposition method. *Journal of Bridge Engineering*, 24(8), Article 06019004. [https://doi.org/10.1061/\(ASCE\)BE.1943-5592.0001458](https://doi.org/10.1061/(ASCE)BE.1943-5592.0001458)
- Zhu, Y., Ni, Y. Q., Jesus, A., Liu, J., & Laory, I. (2018). Thermal strain extraction methodologies for bridge structural condition assessment. *Smart Materials and Structures*, 27(10), Article 105051. <https://doi.org/10.1088/1361-665X/aad5fb>
- Zhu, X. Q., & Law, S. S. (2015). Structural health monitoring based on vehicle-bridge interaction: accomplishments and challenges. *Advances in Structural Engineering*, 18(12), 1999-2015. <https://doi.org/10.1260/1369-4332.18.12.1999>